

# A modified cluster-hadronization model<sup>★</sup>

Jan-Christopher Winter<sup>a</sup>, Frank Krauss<sup>a,b</sup>, Gerhard Soff<sup>a</sup>

<sup>a</sup>*Institut für Theoretische Physik, TU Dresden, D-01062 Dresden, Germany*

<sup>b</sup>*Theory Division, CERN, CH-1211 Geneva 23, Switzerland*

---

## Abstract

A new phenomenological cluster-hadronization model is presented. Its specific features are the incorporation of soft colour reconnection, a more general treatment of diquarks including their spin and giving rise to clusters with baryonic quantum numbers, and a dynamic separation of the regimes of clusters and hadrons according to their masses and flavours. The distinction between the two regions automatically leads to different cluster decay and transformation modes. Additionally, these aspects require an extension of individual cluster-decay channels that were available in previous versions of such models.

*Key words:* QCD, hadronization, hadronization models, hadron production, jet physics, electron-positron annihilation, LEP physics

*PACS:* 13.87.Fh, 12.38.Aw, 13.66.Bc

---

## 1 Introductory note

Multi-hadron and jet production in high-energy particle reactions is a basic property of the strong interaction [1,2]. A successful description relies on a factorization, which permits the separation of the perturbative evolution from the non-perturbative development of an event. The perturbative regime can be characterized through calculations of hard matrix elements and subsequent multiple parton emissions – the physically appealing parton-shower

---

<sup>★</sup> Work supported in part by the EC 5th Framework Programme under contract number HPMF-CT-2002-01663.

*Email addresses:*

winter@theory.phy.tu-dresden.de (Jan-Christopher Winter),

krauss@theory.phy.tu-dresden.de (Frank Krauss),

soff@physik.tu-dresden.de (Gerhard Soff).

picture<sup>1</sup>. However the entire hadron-production mechanism cannot be precisely predicted because of the lack of the understanding of non-perturbative QCD effects, i.e. hadronization. For the transition of a coloured partonic system into colourless primary hadrons, this implies a need for phenomenological models. Lastly, after the primary-hadron genesis, decays of unstable hadrons are accomplished. Employing the separation ansatz, Monte Carlo event generators such as JETSET/PYTHIA [5] or HERWIG [6] proved to be a successful tool for the description of multiparticle generation in high-energy physics.

Concerning the transition process, such Monte Carlo schemes are either based on the Feynman–Field or independent fragmentation [7], on the Lund string [8] and UCLA [9] model (JETSET/PYTHIA), or on the cluster-hadronization model (HERWIG). The latter concept<sup>2</sup>, initially proposed by Wolfram and Field [11,12], and further advanced, among others [13], by Webber and Marchesini [14,15], explicitly rests upon the preconfinement property of QCD [16] and the LPHD hypothesis [17]. Such cluster models are usually formulated in terms of two phases: cluster formation accomplished through the non-perturbative splitting of gluons left by the parton shower into quark–antiquark pairs, and cluster decays leading to the additional creation of light-flavour pairs.

To understand the physics at present and future colliders, e.g. the Tevatron at Fermilab and the LHC at CERN, one fundamental cornerstone is the implementation of new Monte Carlo event generators, e.g. PYTHIA7 [18–20], and HERWIG++ [18,21,22]. The development of the C++ Monte Carlo event generator SHERPA (Simulation of High Energy Reactions of PArticles) [18,23] is a step in the same direction. The modified phenomenological cluster-hadronization model presented in this paper contributes as a further module to the construction of the SHERPA package. The basic features of the new model are:

Soft colour reconnection is accounted for in the formation and decay of clusters. The flavour-dependent separation of the cluster regime from the region of hadron resonances yields the selection of specific cluster-transition modes. The two regimes are distinguished by comparing the mass of the cluster with the masses of the accessible hadrons matching the cluster’s flavour structure. So far, the cluster scheme presented here is implemented only for electron–positron annihilation, and, for simplicity, only the light-quark sector is considered. An extension to heavy quarks, however, is straightforward.

The paper describing our cluster-hadronization model is organized as follows: first, different aspects of cluster formation are discussed in Sec. 2. Subsequently, in Sec. 3, the parametrization of light-flavour pair creation is presented. The model’s description is concluded by exhibiting cluster transformation and fragmentation processes, which lead to the emergence of primary hadrons, see Sec. 4. The first results obtained with the new hadronization scheme are shown in Sec. 5 for the process  $e^+e^- \rightarrow \gamma^*/Z^0 \rightarrow d\bar{d}, u\bar{u}, s\bar{s} \rightarrow$

---

<sup>1</sup> Perturbative QCD cascades can be formulated in two complementary ways, either in terms of quarks and gluons or in terms of colour dipoles [3,4].

<sup>2</sup> Recent developments may be found, e.g. in [10].

hadron jets.

## 2 Cluster formation

The parton shower describes multiple parton emission in a probabilistic fashion [2]. By factorizing the full radiation pattern into individual emissions it employs the large- $N_C$  limit of QCD. This organizes a binary tree, i.e. a planar structure, of the partons. It also ensures that, once the colour structure of the initial partons from the hard matrix element is fixed, the colour structure of the partons at the end of the parton shower is unambiguously determined.

In our model, the non-perturbative transition of these partons into primary hadronic matter, clusters, is accomplished by the following steps:

- (1) To guarantee the independence of the hadronization model from the quark masses eventually used in the parton shower and to account for a gluon mass needed by the model, all partons are brought to their constituent masses [14],  $\mathcal{O}(0.3 \text{ GeV})$ ,  $\mathcal{O}(0.3 \text{ GeV})$  and  $\mathcal{O}(0.45 \text{ GeV})$  for  $u$ ,  $d$  and  $s$  flavours, and  $\mathcal{O}(1 \text{ GeV})$  for the gluon, respectively. For this transition a numerical method, involving several particles and consisting of a series of boosts and scaling transformations, is employed. However, these manipulations are applied only to parton-shower subsets that are in a colour-singlet state.
- (2) Since in cluster-hadronization models the clusters consist of two constituents in a colour-neutral state made up of a triplet–antitriplet, the gluons from the parton shower must split (at least) into quark–antiquark pairs [12]. So, a transition – in principle non-perturbative – transition  $g \rightarrow q\bar{q}$ ,  $\bar{D}D$  into a light quark–antiquark pair  $q\bar{q}$  or a light antiquark–diquark pair  $\bar{D}D$  (see Sec. 3) is enforced for each gluon. The respective flavour composition of the gluon’s decay products is obtained with the same mechanism as used for cluster decays; see Sec. 3. Quarks or diquarks that cannot be produced owing to too high masses are discarded. The kinematical distribution obeys axial symmetry; the energy fraction  $z$  of the quark (antiquark) w.r.t. the gluon is given by a density proportional to  $z^2 + (1 - z)^2$ , i.e. the gluon splitting function<sup>3</sup>. The limits on  $z$  are fixed only after the flavour of the decay products has been selected.
- (3) In contrast to the Webber model of cluster fragmentation [24], our model may also incorporate soft colour reconnection<sup>4</sup> effects by eventually re-arranging the colours of the partons forming the clusters. Starting with a simple cascade, Fig. 1 schematically shows the two options to arrange two

---

<sup>3</sup> Obviously, for antiquark–diquark pairs, this is a simplistic assumption, since it neglects, at least, the different spin structure of diquark production.

<sup>4</sup> Other soft colour reconnection models are presented, e.g. in [25,26].

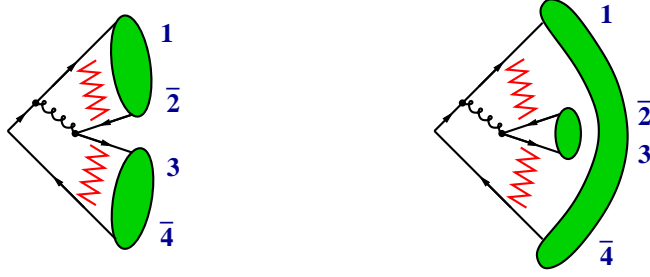


Fig. 1. Both options of cluster formation for a minimal  $qq\bar{q} \rightarrow qq'q'\bar{q}$  cascade. The zig-zag lines connecting the quark lines symbolize the soft exchange of colour quantum numbers, which is responsible for the colour reconnection.

colour neutral clusters out of four quarks or diquarks. The first – direct – case corresponds to the usual cluster formation and reflects the leading term in the  $1/N_C$  expansion. The second – crossed – configuration keeps track of subleading terms. Motivated by the well-known colour suppression of non-planar diagrams w.r.t. planar ones, the relative suppression factor due to colours is taken to be  $1/N_C^2$ . Additionally, a kinematical weight is applied for each of the two possible cluster pairings. For the pairing  $ij, kl$  this weight reads

$$W_{ij,kl} = \frac{t_0}{t_0 + 4(w_{ij} + w_{kl})^2}, \quad (1)$$

where the quantity  $t_0$ , of the order of  $1 \text{ GeV}^2$ , denotes the scale where the parton-shower evolution stops and hadronization sets in. As a measure,  $w_{ij}$  functions such as the invariant mass

$$m_{ij} = \sqrt{(p_i + p_j)^2} \quad (2)$$

of the parton pair (and therefore the cluster), or their relative transverse momentum, similar to the Durham  $k_\perp$  jet-scheme [27]:

$$p_{\perp ij} = \sqrt{2 \min\{E_i^2, E_j^2\} (1 - \cos \theta_{ij})} \quad (3)$$

might be used. The actual colour configuration of the considered system is then chosen according to the combined colour and kinematical weight. Ultimately, this reshuffling is iteratively applied to combinations of two colour-singlet pairs of partons in the colour-ordered chain.

Of course, users who are not interested in colour reconnection have the possibility to switch this option off.

- (4) The cluster formation is accomplished by merging two colour-connected partons, quark or antiquark and antiquark or diquark, into a colourless cluster. In this way, four different types may arise, mesonic ( $q_1 \bar{q}_2$  and  $\bar{D} D'$ ), baryonic ( $q_1 D$ ), and antibaryonic ( $\bar{D} \bar{q}_2$ ) clusters. The total four-momentum of these clusters is just given by the sum of their constituent four-momenta [12].

### 3 Parametrization of light-flavour pair production

In our model the gluon splitting at the beginning of the cluster formation phase and all cluster decays rely on the emergence of light-flavour pairs, see [12,14]. During hadronization, which typically sets in at a scale of 1.0 GeV, there is no possibility for heavy-flavour pair generation [8]. The appearance of baryonic structures is tied to the creation of light diquark–antidiquark pairs<sup>5</sup>. In contrast to the Webber model, in our approach the total diquark spin  $S$  is explicitly considered. Thus,  $q\bar{q}$  and  $\bar{D}_S D_S$ , where  $q \in \{d, u, s\}$  and  $D_S \in \{dd_1, ud_0, ud_1, uu_1, sd_0, sd_1, su_0, su_1, ss_1\}$ , occur as the possible pairs. Apart from their masses influencing their emergence, the created pair functions only as a flavour label. Furthermore, the pair generation is assumed to factorize, i.e. to be independent of the initial flavour configuration. Therefore, the only interest lies in finding suitable pair-production probabilities, i.e. flavour and spin symmetries should be correctly respected and reasonable hadron multiplicities should be finally obtained in the hadron production. In our model a phenomenological parametrization is achieved by employing hypotheses leading to a general “flavour dicing” scheme. This scheme is applied to both regimes, cluster formation and decay. The hypotheses are:

- (1) The emergence of diquarks, i.e. baryons, is suppressed through a factor  $p_B$  with  $0 \leq p_B \leq 1$ .
- (2)  $SU(3)_F$  symmetry is applied, but is assumed to be broken. This is modelled by a strangeness suppression parameter  $p_s$ ,  $0 \leq p_s \leq 1$ , whereas the production of  $u$  and  $d$  flavours is equally probable (strong-isospin symmetry), hence  $p_{u,d} = (1 - p_s)/2$ . As mentioned above,  $p_{c,b} \equiv 0$ .
- (3) Spin and flavour weights: the spin- $S$  diquark states ( $S = 0, 1$ ) get a weight proportional to  $2S + 1$ . Additionally, a combinatorial factor of 2 and 1 is applied, depending on whether different or equal flavours constitute the diquark. But the fact that all states in the baryonic  $SU(3)_F$  octet and decuplet appear equally likely has to be reproduced. This gives rise to extra weights on the individual diquark types. In particular, the combined diquark weights  $w_D^S$  read (up to the baryon suppression factor):

$$w_{D=ud,sd,su}^{S=0} = p_D, \quad w_{D=ud,sd,su}^{S=1} = 3p_D, \quad w_{D=dd,uu,ss}^{S=1} = 4p_D, \quad (4)$$

where

$$p_D = p_{d,u}^{2-n_s} \cdot p_s^{n_s} / (3p_s^2 - 2p_s + 3) \quad (5)$$

and  $n_s$  denotes the number of strange quarks in the diquark.

An approach respecting  $SU(6)$  flavour-spin symmetry instead is currently investigated.

---

<sup>5</sup> Our treatment of diquarks resembles to some extent the one employed in the Lund approach for baryon production [28].

## 4 Cluster transitions into primary hadrons

Once the clusters have been formed, their masses are distributed continuously and independently of the hard process with a peak at low mass. In contrast, the observable hadrons have a discrete mass spectrum and, hence, the clusters must be converted. This is achieved through binary cluster decays and through transformations of individual clusters into single primary hadrons. Our model does not incorporate the subsequent decays of unstable hadrons. To model the cluster transitions, the following assumptions are employed:

- (1) Cluster fragmentation is universal, i.e. independent of the hard process and of the parton shower. The clusters disintegrate locally without impact on other clusters.
- (2) Cluster transitions, i.e. decays as well as transformations, involve only low momentum transfer, of the order of 1 GeV [14], since hadronization effects are supposed to be sufficiently soft and event-shape variables such as the thrust scale inversely with the centre-of-mass energy.
- (3) The regime of clusters is separated from the regime of hadrons according to the flavours of the cluster constituents and the accessible hadron masses. Clusters are supposed to be hadrons, if their mass is below a threshold mass. This bound is given by the maximum of the heaviest hadron with identical flavour content and the sum of the masses of the lightest possible hadron pair emerging in the decay of those clusters.

The last assumption has two consequences, namely that in a first step the newly formed clusters that are already in the hadronic regime have to be transformed into hadrons; in the subsequent binary decays of the remaining clusters, that also the daughter clusters, which fall into the regime of hadron resonances, have to become hadrons immediately.

In both cases, a definite hadron species  $\mathcal{H}$  has to be chosen according to the flavour structure of the considered cluster  $\mathcal{C}$ . Respecting fixed particle properties, this choice is based on hadron wave functions motivated by a non-relativistic quark model. The wave functions are factorized into a flavour- and a spin-dependent part. In our model the flavour part is given for a two-component system in terms of quarks and diquarks. The overlap of this flavour part with the flavour content of the cluster gives rise to a flavour weight. In addition, since spin information is washed out in the clusters [14], the total spin  $J$  of the hadron manifests itself as a corresponding weight. The total spin is given through the coupling of the relative orbital momentum  $L$  with the net spin  $S$  of the valence components. This can be written as  $\vec{J} = \vec{L} + \vec{S}$ . The contributions of states with different orbital momentum  $L$  to the total-spin sum are accounted for by some a-priori weights  $\mathcal{P}_L$ , which enter as model parameters. Taken together, the total flavour-spin weight  $\mathcal{W}$  for a

single hadron reads

$$\mathcal{W}(q_1 s_1, \bar{q}_2 s_2 \rightarrow \mathcal{H}^J(q_1 s_1, \bar{q}_2 s_2)) \sim \frac{|\langle \psi_F(\mathcal{H}^J) | q_1 s_1, \bar{q}_2 s_2 \rangle|^2}{\sum_{\hat{\mathcal{H}}|j=J} |\langle \psi_F(\hat{\mathcal{H}}^J) | q_1 s_1, \bar{q}_2 s_2 \rangle|^2} \cdot \frac{\sum'_{L,S \rightarrow J} |\langle S | s_1 s_2 \rangle|^2 \mathcal{P}_L |\langle J | LS \rangle|^2}{\sum_j \sum'_{\hat{L}, \hat{S} \rightarrow j} |\langle \hat{S} | s_1 s_2 \rangle|^2 \mathcal{P}_{\hat{L}} |\langle \hat{J} | \hat{L} \hat{S} \rangle|^2}. \quad (6)$$

In contrast to  $q_1$  denoting the quarks,  $\bar{q}_2$  stands for antiquarks as well as diquarks. The spins of the two cluster components 1 and 2 are given by  $s_1 = s(q_1)$  and  $s_2 = s(\bar{q}_2)$ , respectively, and  $\langle \psi_F(\mathcal{H}^J) |$  denotes the flavour part of the hadron wave-function<sup>6</sup>. Moreover,  $|\langle j | ls \rangle|^2 = 2j+1 / (\sum_{i=|l-s|, \dots, (l+s)} 2i+1)$  and  $\sum'_{L,S \rightarrow J}$  is an abbreviation denoting a summation over  $L = 0, 1, \dots$  and  $S = |s_1 - s_2|, \dots, (s_1 + s_2)$ , considering the condition that only those terms contribute, where  $|L - S| \leq J \leq (L + S)$  can be fulfilled. Finally, it should be stressed that the second term of Eq. (6) represents only a static model, which accounts for the correct selection of hadrons according to their total spin.

The cluster fragmentation into primary hadrons is performed in two phases:

(I) When the clusters are formed from colour-connected pairs of quarks and diquarks, some of them, because of their comparably low mass, fall into the hadronic regime. Within our framework these clusters are transformed into single hadrons immediately. In doing so, however, some four-momentum is released and has to be absorbed by other clusters. By allowing hadrons with masses lower than the cluster mass only, the momentum transfer is taken to be a mere energy transfer and, therefore, is time-like. This ensures that the absorbing cluster becomes heavier. To fulfil the low momentum-transfer requirement, the already outlined hadron-selection procedure according to the flavour-spin weights  $\mathcal{W}$  is modified through the inclusion of an additional – kinematic – weight, which behaves like

$$\mathcal{W}_{\text{kin.}} = \exp \left[ - \left( \frac{Q^2}{Q_0^2} \right)^2 \right]. \quad (7)$$

In this equation  $Q^2 > 0$  denotes the squared momentum (i.e. energy) transfer, and  $Q_0$  is the scale related to the low momentum-transfer demand. The limit  $Q_0$ , furthermore, depends on the cluster mass and is also employed in the cluster decays; see below. Note that in the Webber model the clusters being too light to decay are identified to be the lightest hadron with identical flavour structure [24]. In comparison with the Webber scheme, the major difference of our approach in the case of single-cluster transitions is the expansion of the hadron-selection procedure.

The cluster compensating the residual four-momentum is selected such that it contains the partner that emerged in the same non-perturbative gluon-splitting process as one of the constituents of the transformed cluster. In turn,

<sup>6</sup> For mesons this also includes the possibility of singlet-octet mixing occurring in hadron multiplets.





Fig. 2. Direct and crossed flavour arrangement and colour flow guaranteeing colour neutrality for each final-state configuration in cluster two-body decays.

clusters, which fall into the hadron regime and contain two leading quarks, are always split non-perturbatively into two clusters containing only one leading constituent. In this context leading partons, however, are only those quarks and antiquarks that directly originate from the perturbative phase, and not from the non-perturbative gluon splitting or from the cluster decays. For the resulting single-leading clusters, then, the same considerations as for the direct transformation to hadrons apply. In case a cluster in the hadron regime is made of a diquark and an antiquark, which is, in principle, possible, it is forced to specifically decay into two mesons. The details on the forced double-leading cluster breakup and the double-diquark cluster decay are outlined below in paragraph (II); see Eq. (8).

(II) Finally all remaining primary and secondary (daughter) clusters have to be split. The mass categorization outlined above automatically yields one of the modes  $\mathcal{C} \rightarrow \mathcal{C}_1\mathcal{C}_2$ ,  $\mathcal{C} \rightarrow \mathcal{C}_1\mathcal{H}_2$ ,  $\mathcal{C} \rightarrow \mathcal{H}_1\mathcal{C}_2$ , or  $\mathcal{C} \rightarrow \mathcal{H}_1\mathcal{H}_2$ . These modes involve the creation of an extra flavour pair according to the ideas illustrated in Sec. 3. Similarly to the cluster-formation phase, then, two flavour configurations for the decay products emerge, namely a direct one and a crossed one; see Fig. 2. Again, the crossed configuration is suppressed by the colour factor  $1/N_C^2$  and the kinematical weight from Eq. (1) using identical measure functions  $w$  and replacing  $t_0$  by  $Q_0^2$ , which again depends on the mass of the decaying cluster. The cluster-decay kinematics, which makes use of the parameter  $Q_0$ , is fixed to be anisotropic. Starting from a mother cluster with constituent momenta  $p_{1,2}^{\mathcal{C}}$ , the new momenta of the decay-products' constituents read [14]

$$p_{1,2} = \left(1 - \frac{Q_0}{M_C}\right) p_{1,2}^{\mathcal{C}}, \quad p_{\bar{f},f} = \frac{Q_0}{M_C} p_{2,1}^{\mathcal{C}}, \quad (8)$$

where  $f$  and  $\bar{f}$  label the momenta of the newly created flavour pair. Hence, for the two cluster arrangements (see Fig. 2) the momenta are given by  $P_{\text{dir.}}^{\mathcal{X}} = p_1 + p_{\bar{f}}$ ,  $P_{\text{dir.}}^{\mathcal{Y}} = p_f + p_2$  in the direct, and  $P_{\text{cross.}}^{\mathcal{X}} = p_1 + p_2$ ,  $P_{\text{cross.}}^{\mathcal{Y}} = p_f + p_{\bar{f}}$  in the crossed case, respectively. To guarantee well-behaved four-momenta in this fission breaking, our model uses a running  $Q_0$  depending on two parameters,  $\hat{Q}_0$  and  $\hat{M}_0$ , with the constraint  $\hat{Q}_0 < \hat{M}_0$ :

$$Q_0(M_C) = \frac{\hat{Q}_0 \cdot M_C}{\hat{M}_0 + M_C} < M_C. \quad (9)$$



Table 1

Different cluster types emerging through cluster breakups. Decay channels indicating a four-quark, i.e. two-diquark, system to become a hadron within the modes  $\mathcal{C} \rightarrow \mathcal{C}_1\mathcal{H}_2, \mathcal{H}_1\mathcal{C}_2, \mathcal{H}_1\mathcal{H}_2$  are vetoed. The four-quark cluster disintegration into two mesons (see the last row of the table) is only available for the mode  $\mathcal{C} \rightarrow \mathcal{H}_1\mathcal{H}_2$ . The occurrence of the two disintegration possibilities is taken to be equally likely.

Cluster		Direct case	Crossed case		Direct case	Crossed case
$q_1\bar{q}_2$	$\xrightarrow{\bar{q}q}$	$q_1\bar{q} + q\bar{q}_2,$	$q_1\bar{q}_2 + q\bar{q}$	$\xrightarrow{D\bar{D}}$	$q_1D + \bar{D}\bar{q}_2,$	$q_1\bar{q}_2 + \bar{D}D$
$q_1D_2$	$\xrightarrow{\bar{q}q}$	$q_1\bar{q} + qD_2,$	$q_1D_2 + q\bar{q}$	$\xrightarrow{D\bar{D}}$	$q_1D + \bar{D}D_2,$	$q_1D_2 + \bar{D}D$
$\bar{D}_1D_2$	$\xrightarrow{\bar{q}q}$	$\bar{D}_1\bar{q} + qD_2,$	$\bar{D}_1D_2 + q\bar{q}$	$\xrightarrow{D\bar{D}}$	$\bar{D}_1D + \bar{D}D_2,$	$\bar{D}_1D_2 + \bar{D}D$
$\bar{D}_1D_2$	$\longrightarrow$	$q_2\bar{q}_1 + q'_2\bar{q}'_1$		$\longrightarrow$	$q_2\bar{q}'_1 + q'_2\bar{q}_1$	

Having fixed the primary kinematics, via Eq. (8), and the combination of flavours and momenta to the new clusters, their masses can be deduced from the squares of their total four-momenta. Then, as stated above, the different decay modes  $\mathcal{C} \rightarrow \mathcal{C}_1\mathcal{C}_2, \mathcal{C}_1\mathcal{H}_2, \mathcal{H}_1\mathcal{C}_2, \mathcal{H}_1\mathcal{H}_2$  are distinguished. All possible decay channels within each mode are comprehensively summarized in Table 1.

- (1) For the case of breakups involving clusters only, i.e. for  $\mathcal{C} \rightarrow \mathcal{C}_1\mathcal{C}_2$ , nothing has to be done in addition.
- (2) If one of the daughter clusters falls into the hadronic regime, i.e. for  $\mathcal{C} \rightarrow \mathcal{C}_1\mathcal{H}_2$  and  $\mathcal{C} \rightarrow \mathcal{H}_1\mathcal{C}_2$ , a suitable hadron has to be selected such that the hadron will be lighter than the cluster. The selection procedure follows the one outlined above for the  $\mathcal{C} \rightarrow \mathcal{H}$  transformation; the recoil is taken by the daughter system, which belongs to the cluster regime.
- (3) If both new clusters fall into the hadron regime, i.e. for purely hadronic decays  $\mathcal{C} \rightarrow \mathcal{H}_1\mathcal{H}_2$ , more severe manipulations are applied. First of all, the newly created flavour pair  $f\bar{f}$  is abandoned; instead, two hadrons are chosen directly. Then the combined weight for the selection of such a hadron pair consists of three pieces. The first part accounts for the two flavour-spin contents. The second one includes the correct relation of direct to crossed decay configurations and, furthermore, represents the incorporation of the pair-production rates. The last part considers the phase space of the decay, which is taken to be isotropic in the cluster's rest frame [12,14]. The combination of the first two weights for the hadron pair is set up as if only complete  $SU(3)_F$  multiplets were accessible. Because of the superposition with the phase-space factor, a hadron pair that cannot be produced in a cluster decay owing to its large mass cannot contribute to the selection<sup>7</sup>. The other manipulation, as indicated above, is that once the hadron species are chosen, the cluster decays isotropically

<sup>7</sup> The weight treatment for hadron selection in HERWIG was modified by Kupčo [29]. However, currently, the HERWIG++ group is working on a new approach [18].

in its rest frame into these hadrons.

Two comments are in order here: first of all, our approach takes leading-particle effects into account in the same manner as in Webber’s model [24]. Secondly, when considering a cluster consisting of two diquarks, mesons can emerge only by recombining the individual quarks and anti-quarks that constitute the diquarks, see Table 1. Since baryons appear in a decay of such clusters through the creation of a quark pair, the diquark recombination is taken to be suppressed by a factor of  $p_B$  w.r.t. the baryon production, which appears with  $1 - p_B$  in this channel. The specific ordering of the quarks into mesons is then done in a fashion similar to the one above, involving hadron pairs. The difference, however, lies in the fact, that Clebsch-Gordan coefficients are additionally employed. These coefficients account for the rearrangement of the diquark spin wave-functions into a double-mesonic basis.

## 5 Preliminary results

The performance of the model introduced above is now illustrated by presenting some results for  $e^+e^-$  annihilation at the  $Z^0$  pole using only light quarks throughout the event’s evolution. The outcomes have been obtained with the parton shower of APACIC++-1.0 [30], the matrix elements are generated by AMEGIC++-1.0 [31] and matched with this parton shower [32], the primary hadronization is accomplished by the cluster model described above, and the hadron decays are provided through interfacing the corresponding routines of PYTHIA-6.1 [33]. The resulting event generator is the combination of these modules. In the following it is referred to as SHERPA $\alpha$ . All results shown below are achieved with the same parameter set, where the cluster-model parameters have been adjusted by hand. The settings of the other module’s input variables are mainly taken over from a tuning of APACIC++-1.0, together with the full hadronization of PYTHIA-6.1. Since measurements that specifically concentrate on the observation of light-quark characteristics are rarely available, our results are mainly compared with those gained from running PYTHIA-6.1 and HERWIG-6.1 [34] both restricted to  $u, d, s$  quarks. Thereby either of the models has been run with its default parameter values.

To begin with, the effects of our colour-reconnection model on the cluster-mass distribution, and the statistics of the reconnections in the cluster formation are briefly discussed. Figure 3 illustrates the statement that under the influence of colour reconnection our cluster hadronization tends to produce less massive primary clusters than without the reconnection procedure. The decrease is especially caused by the kinematical factor, Eq. (1), where  $w_{ij} = p_{\perp ij}$  has been used. In the cluster formation one gets approximately 0.74 reconnections per event and, with a frequency of 48%, 35%, 13%, 3%, and 1%, one

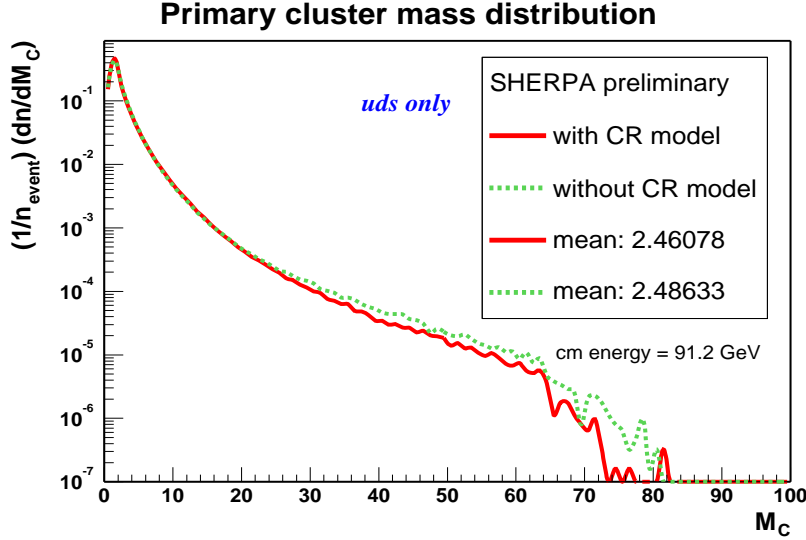


Fig. 3. Primary cluster-mass distribution in electron–positron annihilation events that evolve into light-quark and gluon jets at the  $Z^0$  pole. The SHERPA $\alpha$  result is shown with (solid line) and without (dashed line) colour-reconnection (CR) model.

finds 0, 1, 2, 3, and  $> 3$  exchange(s), respectively. Moreover, switching off the colour-reconnection option entirely while keeping all the other parameters unchanged yields the following qualitative modifications: the number of daughter clusters per event is increased, which results in an enlargement of the mean charged-particle multiplicity of roughly 0.2 tracks per event. The charged-pion production rate increases whereas the charged-kaon rate and the (anti)proton rate decrease. Furthermore, the charged particle transverse-momentum distributions are lowered for high  $p_{\perp}^{\text{in/out}}$ ; however, for the scaled-momentum distribution of charged tracks, see also below, the bump at  $x_p^{uds} \approx 0.5$  enhances and its tail tends to become harder.

The overall charged-particle multiplicity distribution is presented in Fig. 4. The shift to higher multiplicities of the SHERPA $\alpha$  curve w.r.t. the other curves indicates the higher mean value of the SHERPA $\alpha$  prediction. Table 2 shows mean multiplicities  $\langle \mathcal{N}_{\text{ch}}^{uds} \rangle$  as provided by those three fragmentation models in comparison with inclusive measurements. To exemplify the charged hadron rates, the mean multiplicities for the eventually observable charged hadrons –  $\pi^{\pm}$ ,  $K^{\pm}$  and  $p, \bar{p}$  – are considered and compared with experimental  $uds$  results; see also Table 2. In view of these comparisons, one can conclude that the obtained SHERPA $\alpha$  multiplicity results are satisfactory, and in good agreement with the PYTHIA-6.1( $uds$ ) predictions as well as with the data.

As an example for a particle-momentum distribution the scaled momentum  $x_p^{uds} = 2|\vec{p}_{uds}|/E_{\text{cm}}$  and its negative logarithm  $\xi_p^{uds} = -\ln x_p^{uds}$  are considered. The  $x_p^{uds}$  distribution obtained with SHERPA $\alpha$  is shown in Fig. 5, and compared with the predictions of the PYTHIA-6.1( $uds$ ) and HERWIG-6.1( $uds$ ) event generators. Furthermore, experimental results delivered by the OPAL, DELPHI and SLD collaborations on this differential cross section are included. The PYTHIA-6.1( $uds$ ) model is the most consistent with the OPAL and DEL-

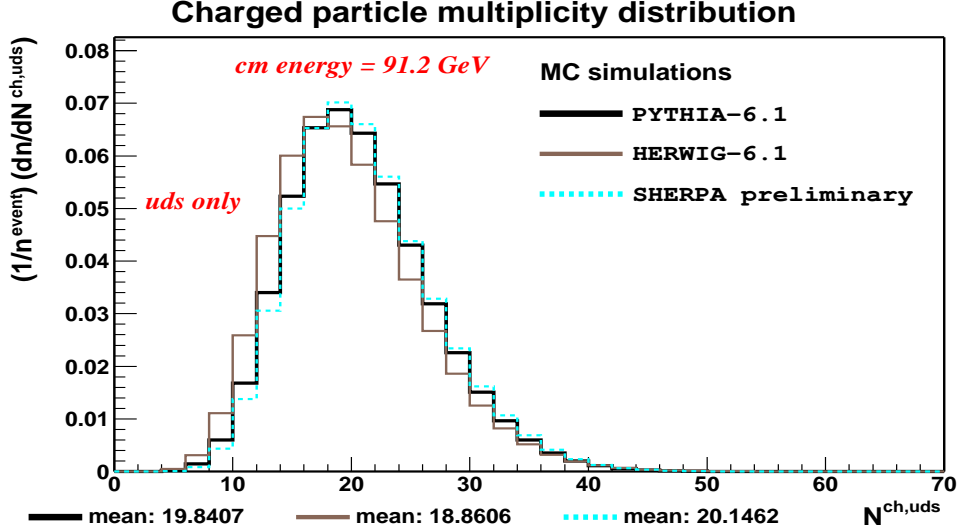


Fig. 4. Predicted multiplicity distribution of charged particles in  $e^+e^-$  annihilation for light-quark and gluon jets at the  $Z^0$  pole. The SHERPA $\alpha$  result is compared with the default PYTHIA-6.1( $uds$ ) and HERWIG-6.1( $uds$ ) predictions.

PHI data, but it predicts a slightly softer spectrum. Both cluster-hadronization models show a similar behaviour concerning their deviation from these data. For  $x_p^{uds} < 0.7$  they wiggle around the PYTHIA-6.1( $uds$ ) prediction and for  $x_p^{uds} > 0.8$  they anticipate a steeper decline, which is quite different from that seen in the OPAL and DELPHI data. However, recently published SLD results on this topic support the tendency of having a much weaker high- $x_p^{uds}$

Table 2

Overall mean charged-particle multiplicity, and production rates of charged pions, charged kaons and (anti)protons in  $e^+e^-$  collisions. The values are taken for  $uds$  events running at the  $Z^0$ -peak centre-of-mass energy. The errors indicated in the table are the total errors of the measurements. The abbreviations PY61( $uds$ ) and HW61( $uds$ ) stand for PYTHIA-6.1( $uds$ ) and HERWIG-6.1( $uds$ ), respectively. More JETSET and HERWIG results on the topic can be found in [35].

	$\langle \mathcal{N}_{ch}^{uds} \rangle$	$\langle \mathcal{N}_{\pi^\pm}^{uds} \rangle$	$\langle \mathcal{N}_{K^\pm}^{uds} \rangle$	$\langle \mathcal{N}_{p,\bar{p}}^{uds} \rangle$
PY61( $uds$ )	19.84	16.72	2.010	0.856
HW61( $uds$ )	18.86	15.37	1.693	1.568
SHERPA $\alpha$	20.15	16.83	2.018	1.047
OPAL [36]	$20.25 \pm 0.39$			
DELPHI [37]	$20.35 \pm 0.19$			
DELPHI [35]	$19.94 \pm 0.34$	$16.84 \pm 0.87$	$2.02 \pm 0.07$	$1.07 \pm 0.05$
SLD [38]	$20.21 \pm 0.24$			
SLD [39]	$20.048 \pm 0.316$	$16.579 \pm 0.304$	$2.000 \pm 0.068$	$1.094 \pm 0.043$

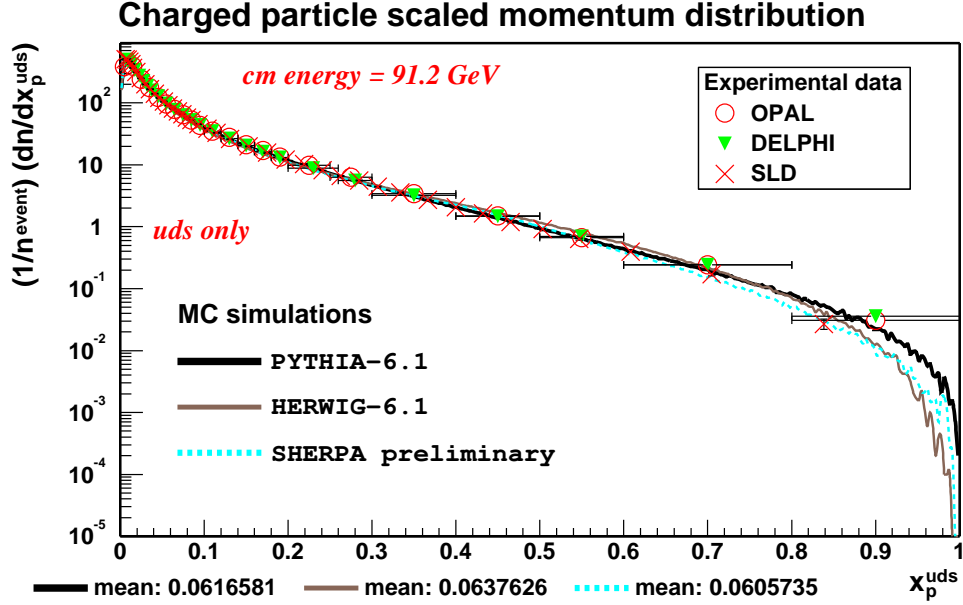


Fig. 5. Scaled momentum distribution of charged particles for  $E_{\text{cm}} = 91.2$  GeV in  $e^+e^-$  annihilation considering only the light-quark sector. The SHERPA $\alpha$  prediction is compared with experimental light-quark data provided by the OPAL, DELPHI and SLD collaborations, and to the PYTHIA-6.1 ( $uds$ ) and HERWIG-6.1 ( $uds$ ) outcomes, using their default settings. Concerning the mean value  $\langle x_p^{uds} \rangle$  of the distributions, only the HERWIG-6.1 ( $uds$ ) prediction is consistent with the OPAL measurement of  $\langle x_p^{uds} \rangle = 0.0630 \pm 0.0003(\text{stat.}) \pm 0.0011(\text{syst.})$  given in [36].

tail. This behaviour then is well described by our cluster model. The hump at  $x_p^{uds} \approx 0.5$  is truly a deficiency of cluster approaches. In comparison with the HERWIG-6.1 ( $uds$ ) prediction, our model yields a smaller bump, and the values for  $x_p^{uds} > 0.9$  do not fall off as rapidly as the HERWIG-6.1 ( $uds$ ) ones. This performance might be due to the mass categorization treatment of the cluster transitions, which has been introduced in our model. All in all, the  $x_p^{uds}$  behaviour clearly reflects two cluster-model weaknesses, namely (1) that the necessary increase in cluster and, therefore, in hadron multiplicity excessively results in a decrease of large three-momenta of primary clusters, and (2) that the hadronization of events with a small number of primary clusters is not sufficiently modelled yet.

In contrast to the  $x_p^{uds}$  distribution, the  $\xi_p^{uds}$  distribution emphasizes the soft momenta of the spectrum. Figure 6 illuminates the SHERPA $\alpha$  result together with those of the other two QCD Monte Carlo models, and compares them with experimental measurements from the OPAL, DELPHI and SLD collaborations. SHERPA $\alpha$  describes the data over most of the  $\xi_p^{uds}$  region, and is in quite good agreement with the PYTHIA-6.1 ( $uds$ ) prediction. It underestimates the region of  $1 < \xi_p^{uds} < 2$ ; on the other hand, however, it slightly overestimates the data for  $3 < \xi_p^{uds} < 5$ . Experimental inclusive measurements of the peak position,  $\xi_p^{*,uds} = 3.76 \pm 0.02$  (DELPHI [35]) and  $\xi_p^{*,uds} = 3.74 \pm 0.22$  (OPAL [36]), seem to be reproduced by the PYTHIA-6.1 ( $uds$ ) and SHERPA $\alpha$  Monte Carlo

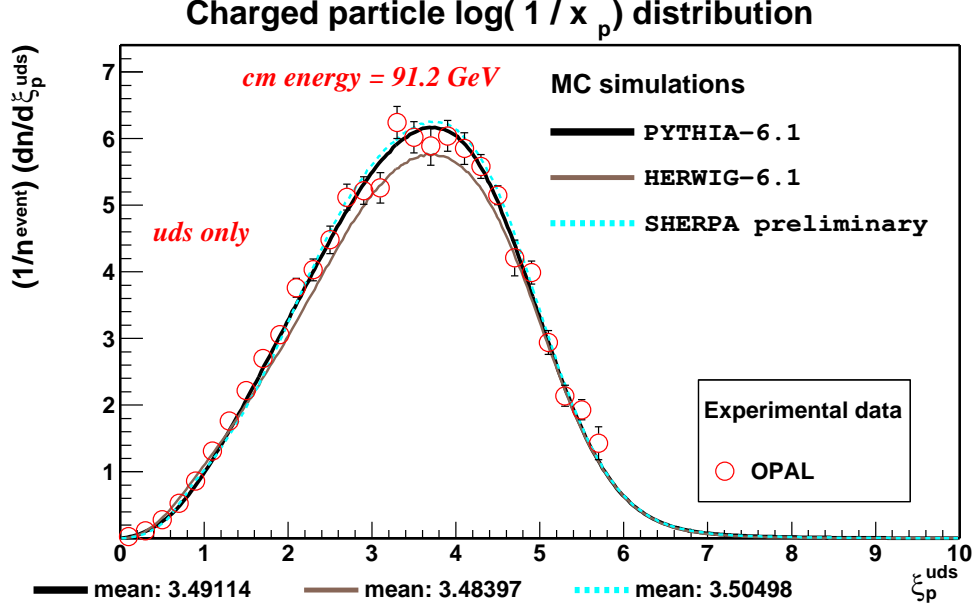


Fig. 6.  $\xi_p^{uds} = \ln(1/x_p^{uds})$  distribution of charged particles for  $E_{cm} = 91.2$  GeV in  $e^+e^-$  annihilation, considering the light-quark sector only. The SHERPA $\alpha$  prediction is presented together with experimental  $uds$  data provided by the OPAL collaboration, and with results from default PYTHIA-6.1( $uds$ ) and default HERWIG-6.1( $uds$ ).

simulations. HERWIG-6.1( $uds$ ) is considerably low (high) for  $2 < \xi_p^{uds} < 5$  ( $0.5 < \xi_p^{uds} < 1$ ).

As an example for the group of event-shape observables, the  $1 - T$  distribution,  $T$  being the thrust, of the three aforementioned QCD Monte Carlo event generators with  $u, d, s$  quark restriction is presented in Fig. 7 for light-quark and gluon jets. HERWIG-6.1( $uds$ ) accounts on average for more spherical event

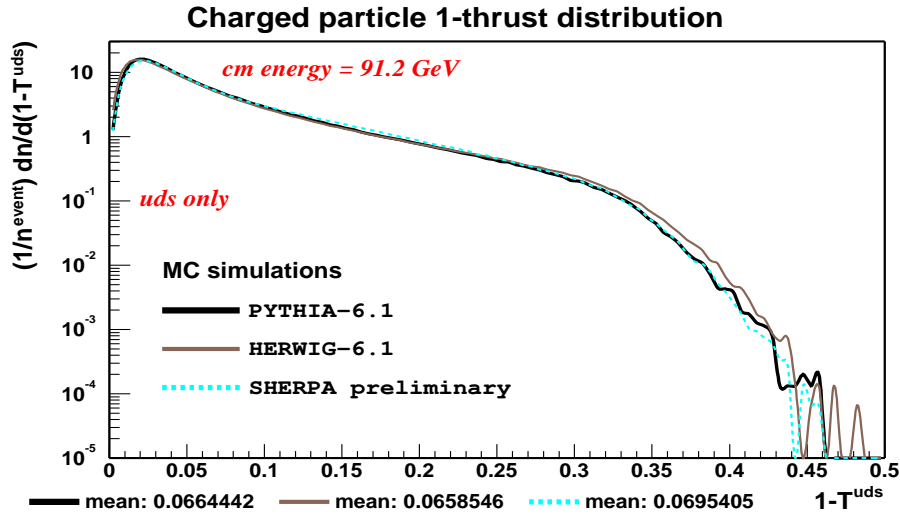


Fig. 7.  $1 - T/x_p^{uds}$  distribution of charged particles for  $E_{cm} = 91.2$  GeV in  $e^+e^-$  annihilation with a restriction on  $u, d, s$  and gluon jets. The SHERPA $\alpha$  prediction is compared with predictions of default PYTHIA-6.1( $uds$ ) and HERWIG-6.1( $uds$ ).

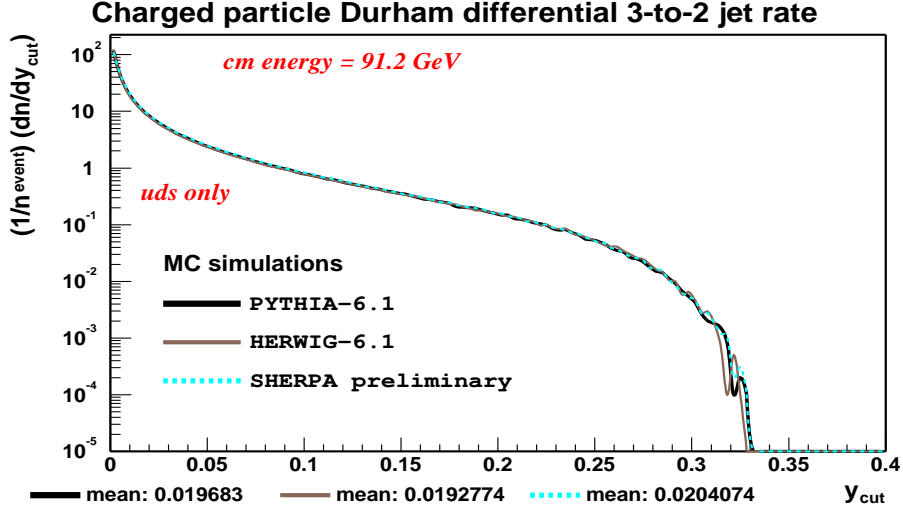


Fig. 8. The Durham  $3 \rightarrow 2$  differential jet rate of charged particles in  $e^+e^-$  annihilation at the  $Z^0$  pole. Only  $uds$  events are taken into account. The SHERPA $\alpha$  result is compared with the results stemming from PYTHIA-6.1( $uds$ ) and HERWIG-6.1( $uds$ ) performances, both of which run with their default parameters.

shapes, which is indicated by a weaker decline of the spectrum towards higher values. Owing to the LPHD concept, the SHERPA $\alpha$  prediction, somewhat exceeding the PYTHIA-6.1( $uds$ ) result for  $0.1 < 1-T < 0.3$ , rather resembles the prediction of PYTHIA-6.1( $uds$ ), which might be due to the fact that SHERPA $\alpha$  employs a PYTHIA-like parton shower.

Lastly the Durham  $3 \rightarrow 2$  differential jet rate is considered in Fig. 8. Except for the low-statistics region, the results for the event generators shown in the plot barely exhibit any deviation from one another.

Taken together, one can conclude that a good performance could be achieved by the new model in electron-positron annihilation into light-quark and gluon jets at the  $Z^0$  pole, although this model has not been sufficiently tuned yet. These first SHERPA $\alpha$  outcomes indicate an encouraging agreement with results obtained from PYTHIA-6.1 restricted onto the light-quark sector. Where provided, the comparison with experimental data is satisfactory.

## 6 Summary and conclusions

A modified cluster-hadronization model has been presented. In comparison with the long-standing Webber model, the extensions of our approach are the following.

Soft colour-reconnection effects are included in the cluster formation as well as in the cluster-decay processes. This yields an enhancement of the number of decay configurations. The spin of diquarks is explicitly accounted for throughout the model. The number of basic cluster species is enlarged, especially by



a new mesonic-cluster type, the four-quark cluster. The significant feature of our approach is the flavour-dependent separation of the cluster and hadron regimes in terms of the mother cluster's mass. This categorization automatically selects the cluster-transition mode. Taken together, these aspects require the set-up of generically new cluster decay channels.

Our cluster-hadronization model is implemented as a C++ code. The resulting version is capable of describing electron-positron annihilation  $e^+e^- \rightarrow \gamma^*/Z^0 \rightarrow d\bar{d}, u\bar{u}, s\bar{s}$  into light-quark and gluon jets. Some first tests were passed (see previous section) and the agreement with PYTHIA-6.1(*uds*) and experimental data is satisfactory. Some cluster-model shortcomings, such as the too low charged-particle multiplicity, could be cured; and the spectrum of the scaled momentum could be improved. The model will soon be completed by including heavy-quark hadronization. Furthermore, the focus of future work is on treating the fragmentation of remnants of incoming hadrons, especially in view of proton-(anti)proton applications (Tevatron and LHC physics).

## Acknowledgements

J.W. and F.K. would like to thank Bryan Webber, Torbjörn Sjöstrand, Rick Field, Leif Lönnblad, Stefan Gieseke, Philip Stevens, Alberto Ribon and Mike Seymour for fruitful and pleasant communication on the subject.

J.W. and F.K. are indebted to Klaus Hamacher and Hendrik Hoeth for valuable discussions, especially on the outcome of the model.

Special thanks go to Suzy Vascotto for carefully reading the manuscript.

J.W. would like to thank the TH division at CERN for kind hospitality during the MC4LHC workshop, where parts of this work were completed.

F.K. acknowledges financial support from the EC 5th Framework Programme under contract number HPMF-CT-2002-01663. The authors are grateful for additional financial support by GSI, BMBF and DFG.

## References

- [1] Y. L. Dokshitzer, V. A. Khoze, A. H. Mueller and S. I. Troian, “*Basics Of Perturbative QCD*”, Gif-sur-Yvette, France: Ed. Frontieres (1991).
- [2] R. K. Ellis, W. J. Stirling and B. R. Webber, “*QCD and Collider Physics*”, Cambridge Monogr. Part. Phys. Nucl. Phys. Cosmol. **8** (1996) 1.
- [3] G. Gustafson, Phys. Lett. B **175** (1986) 453;  
G. Gustafson and U. Pettersson, Nucl. Phys. B **306** (1988) 746;  
B. Andersson, G. Gustafson and L. Lönnblad, Nucl. Phys. B **339** (1990) 393.
- [4] L. Lönnblad, Comput. Phys. Commun. **71** (1992) 15.

- [5] T. Sjöstrand, P. Eden, C. Friberg, L. Lönnblad, G. Miu, S. Mrenna and E. Norrbin, *Comput. Phys. Commun.* **135** (2001) 238 [arXiv:hep-ph/0010017]; T. Sjöstrand, L. Lönnblad and S. Mrenna, arXiv:hep-ph/0108264; T. Sjöstrand, L. Lönnblad, S. Mrenna and P. Skands, arXiv:hep-ph/0308153.
- [6] G. Corcella *et al.*, *JHEP* **0101** (2001) 010 [arXiv:hep-ph/0011363]; G. Corcella *et al.*, arXiv:hep-ph/0210213.
- [7] R. D. Field and R. P. Feynman, *Nucl. Phys. B* **136** (1978) 1; *Phys. Rev. D* **15** (1977) 2590.
- [8] B. Andersson, “*The Lund Model*”, Cambridge Monogr. Part. Phys. Nucl. Phys. Cosmol. **7** (1997) 1.
- [9] C. D. Buchanan and S. B. Chun, *Phys. Rev. Lett.* **59** (1987) 1997; S. B. Chun and C. D. Buchanan, *Phys. Lett. B* **308** (1993) 153; *Phys. Rep.* **292** (1998) 239.
- [10] K. Odagiri, *JHEP* **0307** (2003) 022 [arXiv:hep-ph/0307026]; I. Borozan and M. H. Seymour, *JHEP* **0209** (2002) 015 [arXiv:hep-ph/0207283]; P. Richardson, *JHEP* **0111** (2001) 029 [arXiv:hep-ph/0110108]; F. M. Liu, H. J. Drescher, S. Ostapchenko, T. Pierog and K. Werner, *J. Phys. G* **28** (2002) 2597 [arXiv:hep-ph/0109104]; T. Sjöstrand, O. Smirnova and C. Zacharatou Jarlskog, *Eur. Phys. J. C* **21** (2001) 93 [arXiv:hep-ph/0104118]; V. Berezhinsky and M. Kachelriess, *Phys. Rev. D* **63** (2001) 034007 [arXiv:hep-ph/0009053]; H. J. Drescher, M. Hladik, S. Ostapchenko, T. Pierog and K. Werner, *Phys. Rep.* **350** (2001) 93 [arXiv:hep-ph/0007198]; Q. Wang, G. Gustafson and Q. b. Xie, *Phys. Rev. D* **62** (2000) 054004 [arXiv:hep-ph/9912310].
- [11] S. Wolfram, CALT-68-778, *Largely based on a talk given at 15th Rencontre de Moriond, Les Arcs, France, Mar 9 - 21, 1980.*
- [12] R. D. Field and S. Wolfram, *Nucl. Phys. B* **213** (1983) 65.
- [13] T. D. Gottschalk, *Nucl. Phys. B* **214** (1983) 201 and **239** (1984) 349; T. D. Gottschalk and D. A. Morris, *Nucl. Phys. B* **288** (1987) 729.
- [14] B. R. Webber, *Nucl. Phys. B* **238** (1984) 492.
- [15] G. Marchesini and B. R. Webber, *Nucl. Phys. B* **238** (1984) 1 and **310** (1988) 461; B. R. Webber, in *Proc. of the 19th Int. Symp. on Photon and Lepton Interactions at High Energy, LP99*, ed. J.A. Jaros and M.E. Peskin, *Int. J. Mod. Phys. A* **15S1** (2000) 577 [eConf **C990809** (2000) 577] [arXiv:hep-ph/9912292].
- [16] D. Amati and G. Veneziano, *Phys. Lett. B* **83** (1979) 87; G. Marchesini, L. Trentadue and G. Veneziano, *Nucl. Phys. B* **181** (1981) 335.
- [17] Y. I. Azimov, Y. L. Dokshitzer, V. A. Khoze and S. I. Troian, *Z. Phys. C* **27** (1985) 65.
- [18] See the presentations and talks given at the *MC4LHC Workshop at CERN, Geneva, Switzerland, Jul 7 - Aug 1, 2003*, <http://mlm.home.cern.ch/mlm/mcwshop03/mcwshop.html>.

- [19] M. Bertini, L. Lönnblad and T. Sjöstrand, *Comput. Phys. Commun.* **134** (2001) 365 [arXiv:hep-ph/0006152].
- [20] L. Lönnblad and T. Sjöstrand,  
<http://www.thep.lu.se/~leif/Pythia7/Welcome.html>.
- [21] S. Gieseke, arXiv:hep-ph/0210294.
- [22] S. Gieseke, A. Ribon, M. Seymour, P. Stephens and B. R. Webber,  
<http://www.hep.phy.cam.ac.uk/~gieseke/Herwig++/>.
- [23] T. Gleisberg, F. Krauss, A. Schälicke, S. Schumann and J. Winter,  
<http://www.physik.tu-dresden.de/~krauss/hep/>.
- [24] G. Corcella *et al.*, <http://www.hep.phy.cam.ac.uk/~richardn/HERWIG/herwig65/manual.html>.
- [25] T. Sjöstrand and V. A. Khoze, *Z. Phys. C* **62** (1994) 281 [arXiv:hep-ph/9310242].
- [26] B. R. Webber, *J. Phys. G* **24** (1998) 287 [arXiv:hep-ph/9708463].
- [27] S. Catani, Y. L. Dokshitzer, M. Olsson, G. Turnock and B. R. Webber, *Phys. Lett. B* **269** (1991) 432.
- [28] B. Andersson, G. Gustafson and T. Sjöstrand, *Nucl. Phys. B* **197** (1982) 45; *Phys. Scripta* **32** (1985) 574.
- [29] A. Kupčo, arXiv:hep-ph/9906412.
- [30] R. Kuhn, F. Krauss, B. Ivanyi and G. Soff, *Comput. Phys. Commun.* **134** (2001) 223 [arXiv:hep-ph/0004270].
- [31] F. Krauss, R. Kuhn and G. Soff, *JHEP* **0202** (2002) 044 [arXiv:hep-ph/0109036];
- [32] S. Catani, F. Krauss, R. Kuhn and B. R. Webber, *JHEP* **0111** (2001) 063 [arXiv:hep-ph/0109231].
- [33] T. Sjöstrand, P. Eden, C. Friberg, L. Lönnblad, G. Miu, S. Mrenna and E. Norrbin, *Comput. Phys. Commun.* **135** (2001) 238 [arXiv:hep-ph/0010017].
- [34] G. Corcella *et al.*, arXiv:hep-ph/9912396.
- [35] P. Abreu *et al.* [DELPHI Collaboration], *Eur. Phys. J. C* **5** (1998) 585.
- [36] K. Ackerstaff *et al.* [OPAL Collaboration], *Eur. Phys. J. C* **7** (1999) 369 [arXiv:hep-ex/9807004].
- [37] P. Abreu *et al.* [DELPHI Collaboration], *Eur. Phys. J. C* **6** (1999) 19.
- [38] K. Abe *et al.* [SLD Collaboration], *Phys. Lett. B* **386** (1996) 475 [arXiv:hep-ex/9608008].
- [39] K. Abe *et al.* [SLD Collaboration], arXiv:hep-ex/0310017.